Free-standing kinked nanowire transistor probes for targeted intracellular recording in three dimensions

Published in final edited form as:
Nat Nanotechnol. 2014 February ; 9(2): 142–147. doi:10.1038/nnano.2013.273.

Free-standing kinked nanowire transistor probes for targeted intracellular recording in three dimensions

Quan Qing[1,+], **Zhe Jiang**[1,+], **Lin Xu**[1,2], **Ruixuan Gao**[1], **Liqiang Mai**[2], and **Charles M. Lieber**[1,2,3,*]

[1]Department of Chemistry and Chemical Biology, Harvard University, Cambridge, Massachusetts, 02138, USA

[2]State Key Laboratory of Advanced Technology for Materials Synthesis and Processing, WUT-Harvard Joint Nano Key Laboratory, Wuhan University of Technology, Wuhan 430070, China

[3]School of Engineering and Applied Sciences, Harvard University, Cambridge, Massachusetts, 02138, USA

Abstract

Recording intracellular bioelectrical signals is central to understanding the fundamental behaviour of cells and cell-networks in, for example, neural and cardiac systems[1–4]. The standard tool for intracellular recording, the patch-clamp micropipette[5] is widely applied, yet remains limited in terms of reducing the tip size, the ability to reuse the pipette[5], and ion exchange with the cytoplasm[6]. Recent efforts have been directed towards developing new chip-based tools[1–4,7–13], including micro-to-nanoscale metal pillars[7–9], transistor-based kinked nanowire[10,11] and nanotube devices[12,13]. These nanoscale tools are interesting with respect to chip-based multiplexing, but, to date, preclude targeted recording from specific cell regions and/or subcellular structures. Here we overcome this limitation in a general manner by fabricating free-standing probes where a kinked silicon nanowire with encoded field-effect transistor detector serves as the tip end. These probes can be manipulated in three dimensions (3D) within a standard microscope to target specific cells/cell regions, and record stable full-amplitude intracellular action potentials from different targeted cells without the need to clean or change the tip. Simultaneous measurements from the same cell made with free-standing nanowire and patch-clamp probes show that the same action potential amplitude and temporal properties are recorded without corrections to the raw nanowire signal. In addition, we demonstrate real-time monitoring of changes in the action potential as different ion-channel blockers are applied to cells, and multiplexed recording from cells by independent manipulation of two free-standing nanowire probes.

Separation of a nanoelectronic detector element from much larger interconnections is necessary for internalization of the detector without damaging the cell of interest[1–3,10]. To

[*]To whom correspondence should be addressed. cml@cmliris.harvard.edu.
[+]These authors contributed equally to this work

Author Contributions Q.Q., Z.J. and C.M.L. designed the experiments. Q.Q., Z.J., and L.X. performed experiments. R.G. helped in cardiomyocyte culture experiments. Q.Q., Z.J., L.X. and C.M.L. analyzed data. Q.Q., Z.J. and C.M.L. wrote the paper. All authors discussed the results and commented on the manuscript.

Competing financial interests: The authors declare that they have no competing financial interests.

Additional information: Supplementary information accompanies this paper at www.nature.com/naturenanotechnology. Reprints and permission information is available online at http://npg.nature.com/reprintsandpermissions/. Correspondence and requests for materials should be addressed to C.M.L.

date, all approaches[7–14] have focused on fabricating nanodevices on planar substrates, where the detector protrudes from the surface and target cells are brought into contact with the nanodevices by direct seeding and culture[7–9,14] or manipulation of a culture substrate[10–13] (Fig. 1a). These studies have enabled the demonstration of new nanodevice concepts and multiplexed detection, but also have limitations, including, (i) device positions are determined during chip fabrication and cannot be reconfigured during an experiment, (ii) it is difficult to target specific cells or subcellular regions, and (iii) minimally-invasive *in vivo* measurements are difficult. In comparison, a free-standing probe that can be manipulated in 3D (Fig. 1b) would allow targeting of specific cells cultured on substrates or within tissue, although the manipulator size for such probes will limit multiplexing compared to chip-based methods[2,3]. In this regard, development of a general strategy to present nanoelectronic device elements, such as the kinked silicon nanowire field-effect transistor (nanoFET)[10], in free-standing probe structure could expand substantially the capabilities and applications of these devices in electrophysiology.

The realization of free-standing probes with nanoelectronic device tips requires bridging nano-to-macroscopic length scales in a manner that yields robust electrical and mechanical properties. We focus on meeting these challenges for kinked silicon nanowire nanoFET tips as a general example of a two-terminal active nanoelectronic device. In this case, the nanowire arms of the kinked structure serve as nanoscale connections that must be electrically- and mechanically-connected to the macroscopic handle serving as input/output to measurement electronics. Our free-standing kinked nanowire probe fabrication involves two overall stages (Fig. 2): (1) lithographic patterning of a nanometer-to-millimeter probe-end; and (2) mechanical assembly of the probe-end to a millimeter-to-macroscale probe body.

Key steps in the probe-end fabrication are as follows (Fig. 2a–c; Supplementary Methods). First, kinked Si nanowires with nanoFETs encoded synthetically at the kink tip[15] were selectively deposited on a substrate coated with sacrificial nickel and SU8 photoresist layers (Fig. 2a). A representative optical image (Fig. 2d) shows the resulting kinked nanowire and lithography alignment markers. Second, electron-beam lithography (EBL) and photolithography (PL) were used to define the kinked nanowire tip region and the probe body in the SU8 layer, respectively (Fig. 2b). Fig. 2e shows the kinked nanowire region after these steps. Metal interconnects and top SU8 passivations were fabricated, and a photosensitive protection cap was defined at the tip (Fig. 2c). This cap protects the nanowire tip from capillary forces and contamination during assembly to the probe body and storage prior to cell experiments. Images of a completed probe-end structure (Fig. 2f) show the overall probe structure and protection cap at the wired-up nanowire tip-end. The probe-end structures are easily fabricated in parallel. We process 3×4 arrays of probes on ca. 3×3 cm^2 substrates (Supplementary Fig. S1), and larger arrays could be fabricated using EBL instruments capable of handling larger substrates.

To complete the probe we assemble the probe-end structure to a printed circuit board (Fig. 2g; Supplementary Methods). A silicon microlever shorter than the nanowire/SU8 probe structure was glued to the printed circuit board, and then the probe-end structure, released by Ni underlayer etching, was removed from solution (Fig. 2h), aligned, glued, and electrically-connected to the microlever/printed circuit board. An image of an assembled probe (Fig. 2i) highlights the electrical connection and microlever support; a zoom of the tip region (Fig. 2j) shows the nanowire/SU8/metal interconnect structure and protection cap of the probe end.

We have used the free-standing nanowire probes alone or with a second independent probe to interrogate live cells (Fig. 3a). All measurements were carried out in an inverted microscope with probes mounted in X-Y-Z manipulators and temperature-regulated cell

medium (Fig. 3b). Prior to measurements, the photosensitive protection cap on the nanowire probe-end was removed in solution, and for cell measurements the nanowire end was coated with phospholipid layers as previously described[10–12] (see Supplementary Methods).

A differential interference contrast image showing the ends of a free-standing nanowire probe and patch-clamp micropipette recording from a single cultured cardiomyocyte cell (Fig. 3c) highlights the capability of targeting the nanowire probe to specific cell regions and its smaller tip size compared to a patch-clamp micropipette. The sensitivity of these nanoFET probes was characterized before and after cell measurements so that recorded conductance data can be presented as potential (mV) values (see Supplementary Methods). Representative data recorded in PBS solution (Fig. 3d) yields a sensitivity, 7730 nS/V, similar to previous values for chip-based kinked nanowire devices[10] and the average, 8500 ± 4300 nS/V, for probes in our studies. Significantly, the variation in nanoFET sensitivities before and after cell measurements was <10% and often only ~1%, showing that the probes provide reproducible, quantitative potential data.

Data recorded with a phospholipid-modified free-standing nanowire probe from a spontaneously-beating rat neonatal cardiomyocytes (Fig. 3e) exhibit regular peaks with amplitude (67 mV), duration (260 ms) and shape characteristic[16,17] of intracellular (IC) cardiac action potentials (AP). The IC AP peaks were observed 1–20 s after the phospholipid-modified nanoFET was brought into gentle contact with the cell membrane using 40 nm step resolution of the manipulator, and disappeared when the probe was retracted from the membrane. We were unable to record IC AP signals with unmodified nanoFET probes. These results are consistent with biomimetic membrane fusion[10–13,18], and we note that the high positioning accuracy of our free-standing probes should enable future studies of targeting and internalization with specific ligand/receptor functionalized[19–21] probe tips.

In addition, comparison of IC AP peaks recorded sequentially from three cells using the same nanowire probe (Fig. 3f) shows that these similar AP signals have amplitudes of 51, 46 and 56 mV for cells 1, 2 and 3, respectively. These recorded AP amplitudes are consistent with the average values determined from independent nanoFET and patch-clamp probes, 55 mV ± 16 mV (N = 15) and 58 mV ± 25 mV (N = 13), respectively, on similar cultured cardiomyocytes (DIV3). These results show that our free-standing nanowire probes can be used in multiple measurements on arrays of cells or cell networks, which could improve the efficiency of such studies compared to patch-clamp measurements where the glass pipette is replaced for each try on a new cell.

We have also carried out simultaneous measurements on the same cell using both kinked nanowire and patch-clamp probes (e.g., Figs. 3a, c). In these experiments, we first establish IC recording with patch-clamp in the whole-cell current-clamp mode, and then bring the kinked nanowire probe into contact with the cell to establish the nanoFET IC signal; these data exhibit several key features. First, qualitative inspection of the simultaneous IC AP signals from the nanoFET and patch-clamp (Fig. 3g) show that they are very similar in absolute amplitude (mV) and time-dependent shape. Second, analysis of the signal changes as the nanoFET enters the cell (Fig. 3h) reveals that, there was a ca. −50 mV baseline jump as the nanoFET crosses the cell membrane (triangle, Fig. 3h), and that after this first entry peak, all subsequent AP signals from the nanoFET and patch-clamp (blue and red, respectively, Fig. 3h) overlap ~identically with 65 mV peak amplitude.

A small depolarization (~8 mV) in the resting potential of the patch-clamp was observed as the nanowire probe entered the cell, which is likely due to leakage of the patch electrode membrane seal and not nanoFET leakage as follows. First, the patch clamp recording is

sensitive to the contact between the nanoFET and cell membrane, and we have observed that touching but not penetrating cell membranes with the nanoFET can lead to depolarization and/or loss of patch-clamp signals. Second, independent single probe experiments show that the mean stable AP recording time for the nanoFET probe, 5 min (N = 10), is longer than that for the patch-clamp probe, 2.4 min (N = 11), using the same experimental set-up. Third, extended recording with a nanoFET probe (Supplementary Fig. S2) yields full-amplitude 85 mV AP signals over a 5 min period with <3% loss of signal amplitude, thus demonstrating a high-quality membrane seal and minimal effect on the physiological status of the cell by nanoFET insertion.

Significantly, only two parameters intrinsic to the nanoFET are used to convert probe conductance to local potential: (1) the extracellular conductance baseline, which is assigned zero potential (black arrow, Fig. 3h), and (2) the sensitivity (nS/V) of the nanoFET. Hence, the agreement of both position and shape between the two traces is the first and only direct evidence to date for minimally-invasive intracellular recording by a nanodevice. Moreover, these data clearly differentiate our nanoelectronic probes from other intracellular-like recordings based on high seal resistance around extracellular electrodes and localized electroporation[7–9,22]. In addition, the average amplitude of the APs, 55 mV ± 16 mV (nanoFET, N = 15)/58 mV ± 25 mV (patch clamp, N = 13), and rest potentials, −37 mV ± 10 mV (nanoFET)/−43 mV ± 13 mV (patch clamp) obtained from single probe recording experiments are statistically indistinguishable. Last, the highest amplitudes of APs reach 90 mV (Supplementary Fig. S3) thus confirming the high quality of the nanoFET/cell membrane junctions.

Our free-standing kinked nanowire probes were also used to characterize quantitatively the effects of ion channel blockers on recorded IC APs. First, the L-type Ca^{2+} channel blocker nifedipine was injected into the medium after stable IC AP recording was established from a cardiomyocyte cell. Monitoring of the nanoFET signal (Fig. 3i) shows a constant AP peak amplitude and progressive decrease in the full-width at half-maximum (FWHM): 147, 130, and 102 ms at times 0, 60 and 110 s, respectively, after nifedipine injection. The decrease in AP peak FWHM at constant peak amplitude are consistent with a decrease in Ca^{2+} current due to nifedipine binding[23]. Second, addition of Na^{+} channel blocker tetrodotoxin (TTX) monitored in a separate experiment (Fig. 3j) shows a rapid decrease in the initial fast rising (depolarization) edge and corresponding decrease in the peak amplitude of the AP versus time. The slopes (V/s)/peak amplitudes (mV) were 3.42/44, 1.73/28, 0.78/20 and 0.53/13 for 0, 3, 12 and 22 s, respectively, after TTX addition, and are consistent with the suppression of the inward Na^{+} current due to TTX binding[23]. These results confirm that nanoFET probes record details of intracellular AP changes in a reliable and robust manner, and show that it can be a tool for drug screening and cell signaling studies in the future.

Last, we explored using two nanoFET probes in multiplexed recording experiments. For example, two distinct nanoFET probes mounted on independent manipulators (Fig. 4a) have been used to precisely target cultured cardiomyocyte cells, including two adjacent cells with well-defined alignment (Fig. 4b) and a single cell (Fig. 4c). Targeting with submicron resolution was readily achieved using differential interference contrast imaging, and could be improved further using fluorescence imaging. Representative data recorded from two nanoFET probes as they are sequentially brought into contact and internalized by two adjacent cardiomyocytes (Fig. 4d) highlights several key points. First, following gentle contact of the phospholipid-modified probes with the cell (40 nm step resolution), both probes show a short, ~2 s time delay before IC AP peaks appear, with stable full-amplitude APs developing after several additional seconds. Second, the full-amplitude APs recorded with probe-1 and probe-2, 50 and 45 mV, respectively, are consistent with independent patch-clamp measurements and literature[24] for neonatal (vs. adult) cardiomyocytes. The

extracellular to IC baseline shifts can also be smaller for these neonatal cells (i.e., −20 mV/probe-2 versus −43 mV/probe-1) but are consistent with the stage of our neonatal cell culture[24]. These multiplexed studies further highlight the robustness of our free-standing nanowire probe fabrication, and the potential to characterize AP timing differences for precisely defined nanoprobe/cell configurations and structures too small for conventional patch clamp measurements, such as dendritic spines[25]. Moreover, the capability to specify with high-resolution the specific cells/cellular regions targeted by the nanoFET detectors represents an advantage compared to multiplexed recording with nanoelectronic probes fabricated on planar substrates. The physical dimensions of the manipulators used for targeting nanoFET probes will limit level of multiplexing compared to chip-based methods[2,3], although future studies incorporating kinked nanowire structures with synthetically-encoded multiple nanoFET sensors[26] could mitigate this by increasing the number of detectors on each probe.

In summary, we have demonstrated a robust approach for fabrication of free-standing silicon kinked nanowire probes with encoded nanoFET detectors at the tip ends. These probes have been manipulated in 3D with submicron precision to target specific cells/cell regions, and record stable full-amplitude APs from spontaneously beating cardiomyocytes. Simultaneous measurements from the same cell made with kinked nanowire and patch-clamp probes show that the same AP amplitude and temporal properties are recorded without corrections to the raw nanowire signal, thus demonstrating the first direct evidence for minimally-invasive, true IC recording by a nanodevice. In addition, we demonstrated real-time monitoring of AP changes as different ion-channel blockers are added to cells, and multiplexed recording from adjacent cells with precisely-defined alignment and separation using two independent nanoFET probes. The signal-to-noise ratio of our single nanoFET probe, ca. 100, is comparable to or smaller than vertical nanowire (~100[8] and ~590[7]) arrays, although the effective areas of these passive nanoprobes are >50 times larger than our nanoFET probes. Hence, a direct comparison of signal and noise between these experiments is difficult to make because the signal and bandwidth will be substantially degraded for these other devices when reduced to the same size as our current nanoFET probes.

While future studies will be needed to extend the performance and biochemical functionality of our free-standing nanowire probes, we believe this work opens up a number of interesting directions. First, our general approach for fabricating free-standing probes could be applied to other nanoelectronic building blocks that have been used in chip-based format[11–13,26]. For example, the use of U-shape kinked nanowire structures would yield ultra-small nanoFET detectors with very high aspect ratio[26], and thus enhance capabilities for specific targeting, multiplexed experiments, and deep tissue/cell insertion and detection with subcellular resolution. Second, the small detector size and absence of ion-exchange for our nanowire probes could facilitate studies of high input impedance cells such as cystic artery[27], fibroblasts[28], and glial cells[29]. There are also areas where the nanoFET probes are currently limited compared to patch-clamp technology, including the capability to stimulate APs and deliver molecular and/or macromolecular reagents. Last, we believe that our approach could be scaled-up in the future to make these novel 3D nanoelectronic probes accessible to a broad range of users in electrophysiology, bioelectronics and related fields.

Methods Summary

Kinked silicon nanowires with nanoFETs encoded near the kink were synthesized using gold nanocluster catalyzed vapor-liquid-solid growth method as previously described[15]. Probe fabrication was carried out on Si substrates (Nova Electronic Materials, Flower Mound, TX) with 600 nm SiO_2 coated with 100 nm Ni, which serves as relief layer, and pre-baked (65 °C for 2 min) SU8 2000.5 photoresist. Kinked nanowires were deposited on

desired region from ethanol dispersion using a micropipette, and then EBL was used to define nanowire end of the probe and PL used to pattern the remainder of the 4.5 mm long SU8 probe body, which also serves as lower passivation of metal interconnects. Subsequently, a combination of EBL and PL steps were used to define the metal connections scaling from the kinked nanowire arms to the millimeter-scale end of the probe, where Cr/Pd/Cr (1.5/120/60 nm) was used for contacts to the nanowire, and Cr/Au (5/200 nm) for the rest of the interconnections. Top SU8 passivation/structural layers were defined using a 500 nm thick SU8 2000.5 for the tip region covering the metal contacts, and a 50 μm thick low-stress SU8 layer (GLM 2060, Gersteltec) for the majority of the probe body, which can increase the overall mechanical strength. The kinked nanowire end of the probe was protected with 300 and 500 nm thick layers of LOR 3A and S1805 (MicroChem) defined by PL. After etching the Ni layer (40% $FeCl_3$:39% HCl:H_2O=1:1:20), the floating probe structure was removed using tweezers and glued on the printed circuit board connector portion of the probe body that is mounted in the 3D manipulator. The protective cap is removed immediately prior to measurements following UV exposure, and measurements were made in similar manner to previous chip-based device studies[10–11]. Additional fabrication details, as well as cell culture and measurement protocols are described in the Supplementary Information.

Supplementary Material

Refer to Web version on PubMed Central for supplementary material.

Acknowledgments

C.M.L. acknowledges support of this work by a NIH Director's Pioneer Award 5DP1OD003900.

References

1. Parpura V. Bionanoelectronics: Getting close to the action. Nature Nanotech. 2012; 7:143–145.
2. Spira M, Hai A. Multi-electrode array technologies for neuroscience and cardiology. Nature Nanotech. 2013; 8:83–94.
3. Duan, X.; Fu, T-M.; Liu, J.; Lieber, CM. Nano Today. ASAP; 2013. Nanoelectronics-biology frontier: From nanoscopic probes for action potential recording in live cells to three-dimensional cyborg tissues.
4. Dunlop J, Bowlby M, Peri R, Vasilyev D, Arias R. High-throughput electrophysiology: an emerging paradigm for ion-channel screening and physiology. Nature Rev. Drug Discov. 2008; 7:358–368. [PubMed: 18356919]
5. Molleman, A. Patch Clamping: An Introductory Guide to Patch Clamp Electrophysiology. Wiley; 2003.
6. Sakmann, B.; Neher, E. Single-channel recording. New York: Plenum Press; 1995. Ch 2.
7. Xie C, Lin Z, Hanson L, Cui Y, Cui B. Intracellular recording of action potentials by nanopillar electroporation. Nature Nanotech. 2012; 7:185–190.
8. Robinson JT, et al. Vertical nanowire electrode arrays as a scalable platform for intracellular interfacing to neuronal circuits. Nature Nanotech. 2012; 7:180–184.
9. Hai A, Shappir J, Spira ME. Long-term, multisite, parallel, in-cell recording and stimulation by an array of extracellular microelectrodes. J. Neurophysiol. 2010; 104:559–568. [PubMed: 20427620]
10. Tian B, et al. Three-dimensional, flexible nanoscale field-effect transistors as localized bioprobes. Science. 2010; 329:830–834. [PubMed: 20705858]
11. Jiang Z, Qing Q, Xie P, Gao RX, Lieber CM. Kinked p-n junction nanowire probes for high spatial resolution sensing and intracellular recording. Nano Lett. 2012; 12:1711–1716. [PubMed: 22309132]

12. Duan XJ, et al. Intracellular recordings of action potentials by an extracellular nanoscale field-effect transistor. Nat. Nanotechnol. 2012; 7:174–179. [PubMed: 22179566]
13. Gao RX, et al. Outside looking in: nanotube transistor intracellular sensors. Nano Lett. 2012; 12:3329–3333. [PubMed: 22583370]
14. Tian B, et al. Macroporous nanowire nanoelectronic scaffolds for synthetic tissues. Nat. Mater. 2012; 11:986–994. [PubMed: 22922448]
15. Tian B, Xie P, Kempa TJ, Bell DC, Lieber CM. Single-crystalline kinked semiconductor nanowire superstructures. Nat. Nanotechnol. 2009; 4:824–829. [PubMed: 19893521]
16. Bers DM. Cardiac excitation-contraction coupling. Nature. 2002; 415:198–205. [PubMed: 11805843]
17. Zipes, DP.; Jalife, J. Cardiac Electrophysiology: From Cell to Bedside. ed. 2. Saunders: Philadelphia; 2009.
18. Chernomordik LV, Kozlov MM. Mechanics of membrane fusion. Nat. Struct. Mol. Biol. 2008; 15:675–683. [PubMed: 18596814]
19. Nicolas J, Mura S, Brambilla D, Mackiewicz N, Couvreur P. Design, functionalization strategies and biomedical applications of targeted biodegradable/biocompatible polymer-based nanocarriers for drug delivery. Chem. Soc. Rev. 2013; 42:1147–1235. [PubMed: 23238558]
20. Subbiah R, Veerapandian M, Yun KS. Nanoparticles: functionalization and multifunctional applications in biomedical sciences. Curr. Med. Chem. 2010; 17:4559–4577. [PubMed: 21062250]
21. Kotov NA, et al. Nanomaterials for Neural Interfaces. Adv. Mater. 2009; 21:3970–4004.
22. Hai A, Shappir J, Spira ME. In-cell recordings by extracellular microelectrodes. Nature Methods. 2010; 7:200–202. [PubMed: 20118930]
23. Szentandrassy N, et al. Powerful technique to test selectivity of agents acting on cardiac ion channels: the action potential voltage-clamp. Curr. Med. Chem. 2011; 18:3737–3756. [PubMed: 21774754]
24. Viatchenko-Karpinski S, et al. Intracellular Ca^{2+} oscillations drive spontaneous contractions in cardiomyocytes during early development. Proc. Natl. Acad. Sci. U. S. A. 1999; 96:8259–8264. [PubMed: 10393982]
25. Davie JT, et al. Dendritic patch-clamp recording. Nat. Protocols. 2006; 1:1235–1247.
26. Xu L, et al. Design and synthesis of diverse functional kinked nanowire structures for nanoelectronic bioprobes. Nano Lett. 2013; 13:746–751. [PubMed: 23273386]
27. Akbarali HI, Wyse DG, Giles WR. Ionic currents in single cells from human cystic artery. Circ. Res. 1992; 70:536–545. [PubMed: 1371429]
28. Chilton L, et al. K^+ currents regulate the resting membrane potential, proliferation, and contractile responses in ventricular fibroblasts and myofibroblasts. Am. J. Physiol. Heart Circ. Physiol. 2005; 288:H2931–H2939. [PubMed: 15653752]
29. Clark BA, Mobbs P. Voltage-gated currents in rabbit retinal astrocytes. Eur. J. Neurosci. 1994; 6:1406–1414. [PubMed: 8000565]

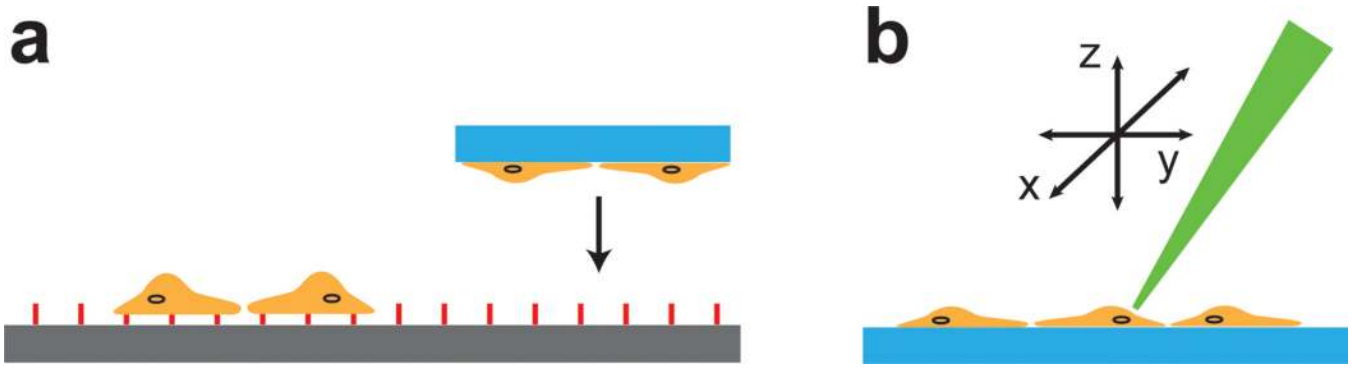

Figure 1. Intracellular recording methods

a, Schematics (side view) of typical recording approach using chip-based device arrays (red) anchored on a planar substrate (grey). Cells (yellow) are usually cultured directly on top of the devices or cultured on a separate substrate (blue), which would be moved into contact with the devices. **b**, Schematics of a free-standing probe, where the probe (green) moves freely in 3D space to target selected cells/cell regions.

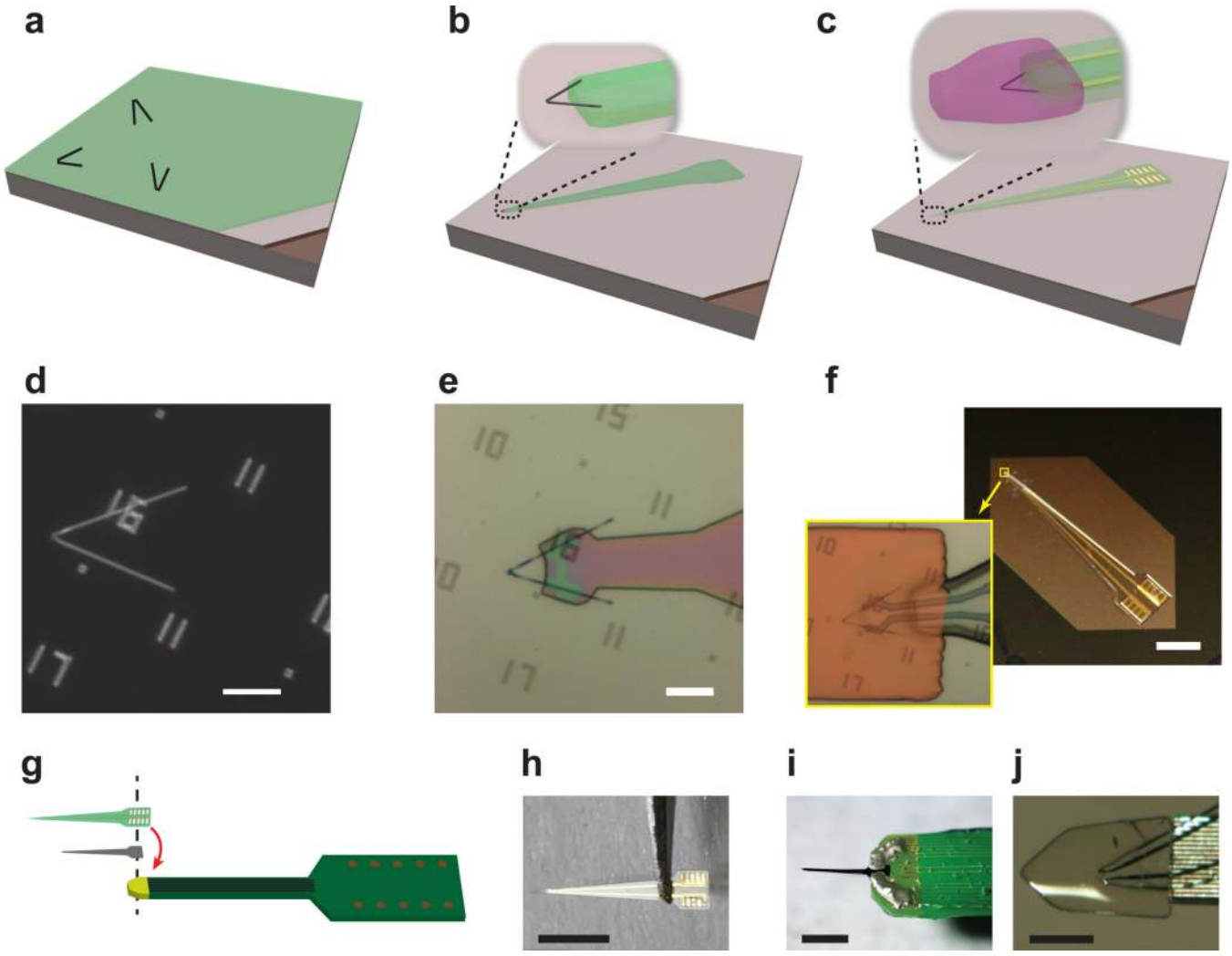

Figure 2. Fabrication and assembly of free-standing nanowire probes

a, Si substrate with 600 nm SiO_2 on surface (brown) coated with a Ni sacrificial layer (pink) and a SU8 polymer layer (light green), and showing deposited kinked silicon nanowires (black). **b**, Kinked nanowire with desired orientation was identified and fixed on the substrate by EBL (inset), and bottom structure/passivation layer for the full probe body (light green) was defined by PL. **c**, Metal connections (golden) from the nanowire to the macroscopic contact pads, and top passivation layers were fabricated by EBL and PL steps (light green), and then the nanowire was protected by an additional photoresist cap (inset, red). **d**, Dark-field optical image showing a selected kinked nanowire on top of the SU8 layer, as well as the metal alignment markers below the SU8 layer, which are used in registration of subsequent lithography steps. Scale bar: 10 μm. **e**, Bright-field optical image of the tip-end highlighting the kinked silicon nanowire and the underlying patterned SU8 probe body. Scale bar: 10 μm. **f**, Digital camera image of a fully fabricated probe on the Ni sacrificial layer. Scale bar: 1 mm. Inset: Bright-field optical image of the probe tip with the photoresist protection cap over the nanowire device. The photoresist protection cap is false-coloured in red for clarity. Scale bar: 10 μm. **g**, Schematic of the assembly of a probe onto a printed circuit board connector body (yellow and dark green). A thin Si lever support (grey) was first glued on the printed circuit board connector, and then the nanowire/SU8 probe body (light green) was aligned and attached on top. The length of the polymer probe is

longer than the Si lever so that the kinked nanowire is fully suspended. Sizes are not to scale for clarity. **h**, Digital camera image of the nanowire/SU8 probe body released from the substrate after etching. Scale bar: 2 mm. **i**, Digital camera image of the fully assembled probe on the printed circuit board connector. Scale bar: 2 mm. **j**, Bright-field optical image of the suspending nanoFET probe on top of the Si lever with the photoresist protection cap. Scale bar: 100 μm.

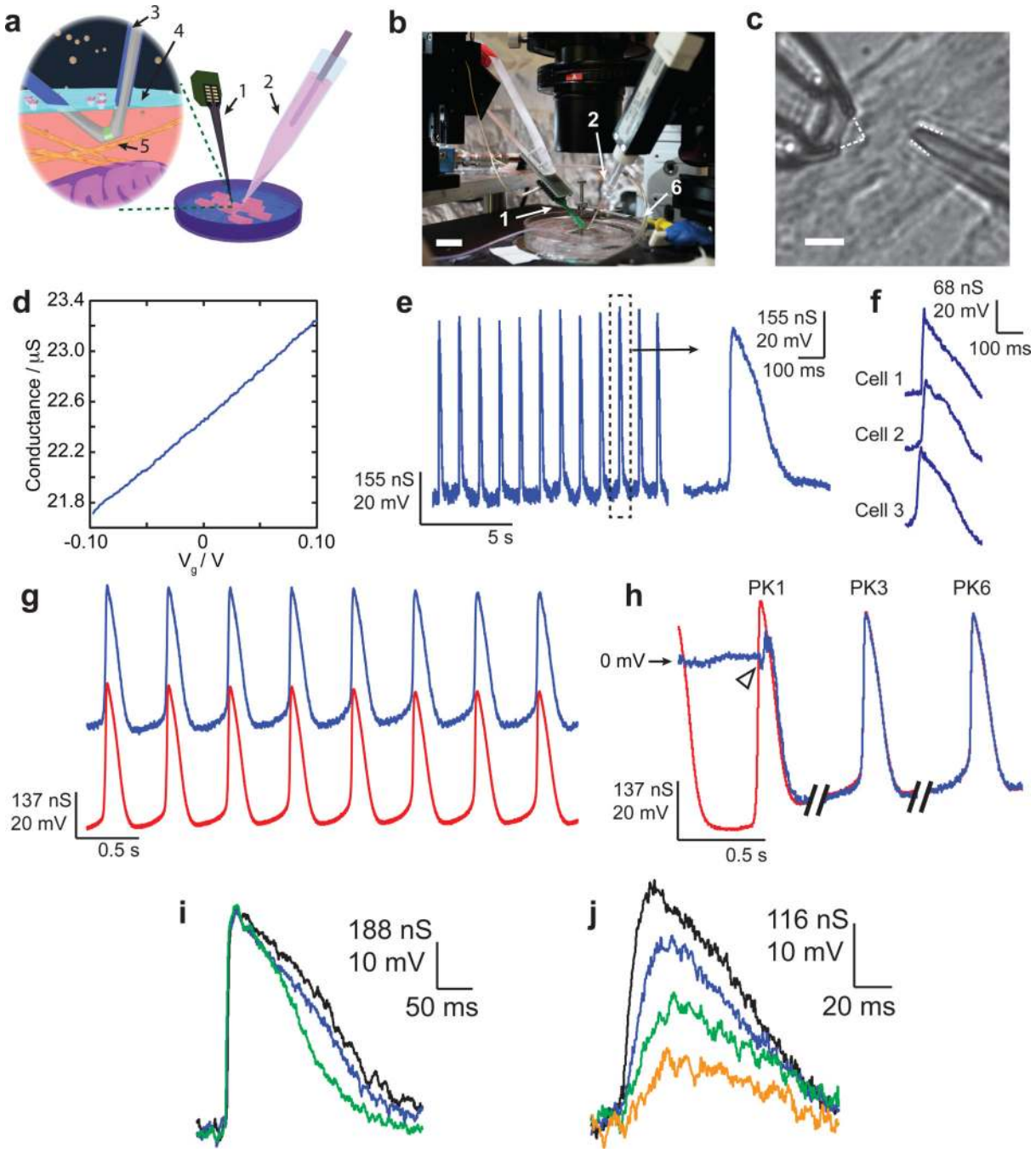

Figure 3. Intracellular recording using free-standing nanowire probes

a, Schematic illustrating general experiment setup. A free-standing nanowire probe (1) is mounted on an x-y-z micromanipulator to target selected cells and record intracellular signals, while a patch-clamp pipette (2), which is also mounted on a manipulator, can be used to monitor the same cell simultaneously. The nanowire is coated with a phospholipid layer (3) to facilitate penetration through the cell membrane (4) so that the nanoFET (5) is inside the cytoplasm. **b**, Digital camera image of the experiment setup where free-standing nanowire (1) and patch-clamp (2) probes are visible. A Ag/AgCl reference (water-gate) electrode (6) is used as reference. Scale bar: 2 cm. **c**, Differential interference contrast image

of the kinked nanowire probe (left) and patch-clamp pipette (right) recording from the same cell. Scale bar: 5 μm. The white dashed lines highlight the kinked nanowire and micropipette inner diameter. **d**, Conductance vs. water-gate data for a typical free-standing nanowire probe recorded with source/drain voltage of 0.1 V. **e**, IC APs recorded from a spontaneously beating cardiomyocyte using the nanoFET probe (blue). Right: Zoom-in of a single AP. **f**, Representative IC AP peaks recorded from three different cells using the same probe consecutively; the probe was not cleaned between trials. **g**, Simultaneous data recorded by a free-standing nanowire probe (blue) and patch-clamp (red, current-clamp mode, $I_{clamp}=0$) from the same spontaneously beating cardiomyocyte. Signals are offset vertically for clarity. **h**, Raw signals recorded from the nanoFET probe (blue) and the patch-clamp (red) as the nanoFET approaches the cell. The triangle marks the time when the nanoFET enters the cell. PK1, PK3 and PK6 mark the 1^{st}, 3^{rd} and 6^{th} AP peaks, respectively. **i**, IC AP peaks recorded from nanoFET at 0 s (black), 60 s (blue), and 110 s (green) after adding 5 μL of 10 mM nifedipine (DMSO solution) to the medium. **j**, IC AP peaks recorded from nanoFET at 0 s (black), 3 s (blue), 12 s (green) and 22 s (orange) after adding 1 mL of 1 mM TTX aqueous solution to the medium.

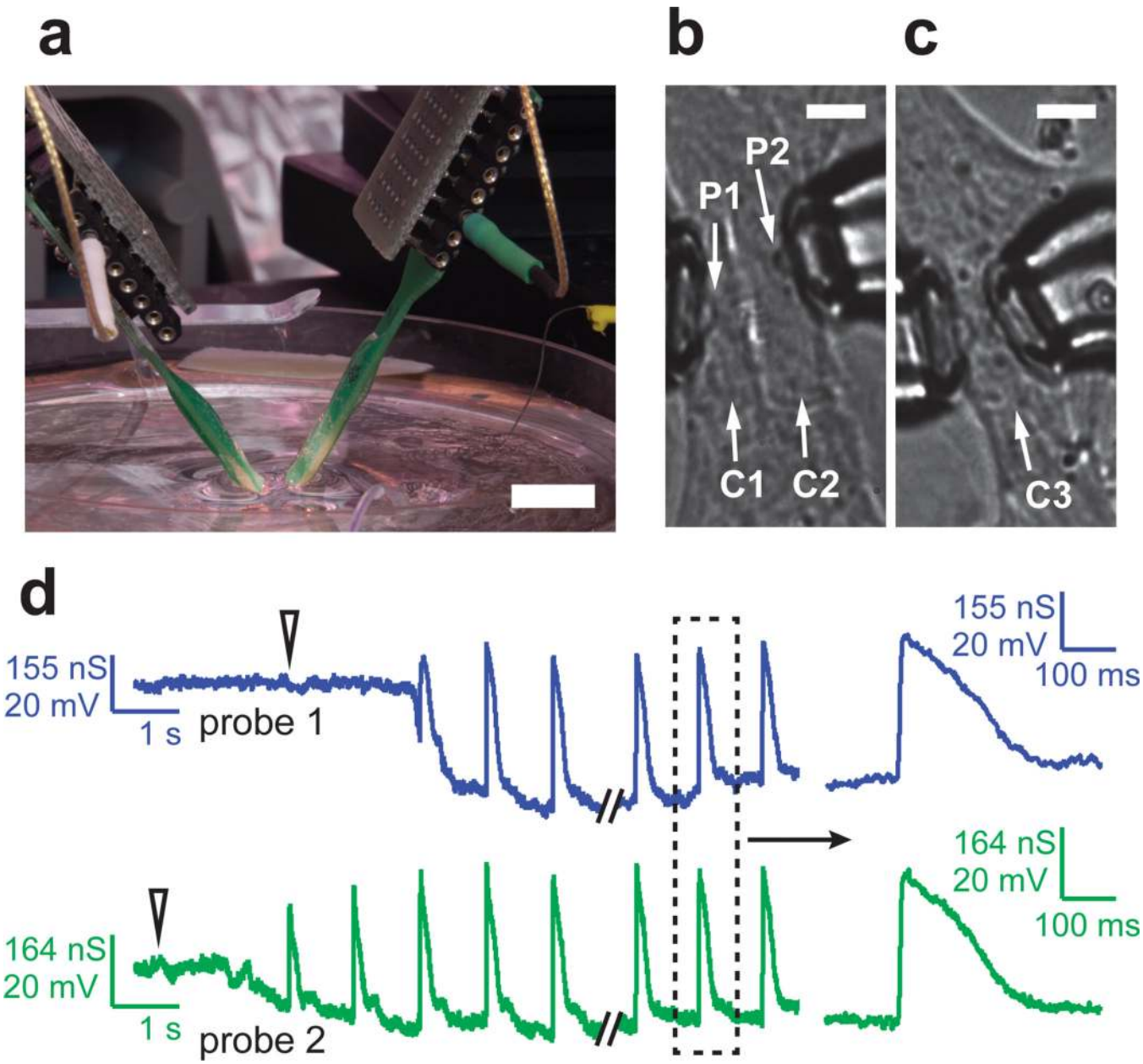

Figure 4. Multiplexed recording with free-standing nanowire probes

a, Digital camera image of a measurement setup using two independent free-standing nanowire probes, where each probe is mounted on an independent x-y-z micromanipulator. Scale bar: 1 cm. **b,c**, Differential interference contrast images of the kinked nanowire probes during multiplexed recording. **b:** Probes P1 and P2 are positioned at two adjacent cardiomyocytes C1 and C2, respectively. **c:** The two probes are positioned within submicron separation on the same cardiomyocyte cell, C3. Scale bars in **b,c**: 10 μm. **d**, Left: Multiplexed IC APs recorded with the dual-kinked nanowire probe setup from two adjacent cardiomyocytes. The triangles mark the time of contact between the nanowire tips and the cells. Right: Zoom-in of the APs marked by the dashed box at left.